Semileptonic decays $B/B_s \to (D^{(*)}, D_s^{(*)})l\nu_l$ in the PQCD approach with the lattice QCD input*

Xue-Qing Hu(胡学卿)[1;1]   Su-Ping Jin(金苏平)[1;2]   Zhen-Jun Xiao(肖振军)[1,2;3]

[1]Department of Physics and Institute of Theoretical Physics, Nanjing Normal University, Nanjing 210023, China
[2]Jiangsu Key Laboratory for Numerical Simulation of Large Scale Complex Systems, Nanjing Normal University, Nanjing 210023, China

Abstract: We study the semileptonic $B/B_s \to (D^{(*)}, D_s^{(*)})l\nu_l$ decays in the framework of the Standard Model (SM), by employing the perturbative QCD (PQCD) factorization formalism combined with the lattice QCD input for the relevant transition form factors. We calculate the branching ratios $\mathcal{B}(B_{(s)} \to D_{(s)}^{(*)}l\nu_l)$ with $l = (e, \mu, \tau)$, the ratios of the branching fractions $R(D^{(*)})$ and $R(D_s^{(*)})$, and the physical observables $P_\tau(D_{(s)}^{(*)})$, $F_L(D_{(s)}^*)$ and $A_{FB}(\tau)$. The "PQCD+Lattice" predictions for $\mathcal{B}(B \to D^{(*)}l\nu_l)$ and $R(D^{(*)})$ agree with the available experimental measurements within errors. For the ratios $R(D_s)$ and $R(D_s^*)$, the "PQCD+Lattice" predictions agree with the other predictions. For $P_\tau(D^*)$ and $F_L(D^*)$, our theoretical predictions agree with the measured values within errors. Our theoretical predictions of the semileptonic B/B_s decays considered could be tested in the near future by the LHCb and Belle II experiments.

Keywords: semileptonic decays, form factor, PQCD, B_s meson

1   Introduction

The studies of semileptonic decays of B/B_s meson play an essential role in testing the Standard Model (SM) as well as in the search for new physics (NP) beyond SM, since the lepton flavor universality (LFU) can be examined in this kind of decay modes. LFU implies that all electroweak gauge bosons (Z^0, γ and $W^\pm$) have equivalent couplings to the three generations of leptons, and the only difference arises from the mass differences: $m_e < m_\mu \ll m_\tau$. Therefore, if the experiments were to find signals of lepton flavor violation (LFV), that would be a true challenge for SM.

The first observation of the $R(D)$ and $R(D^*)$ anomalies in semileptonic decays $B \to D^{(*)}l\nu_l$ with $l^- = (e^-, \mu^-, \tau^-)$ by the BaBar collaboration in 2012 [1, 2] invoked intensive studies of the $B \to D^{(*)}l\nu_l$ decays in the SM framework [3–10] and various NP models [11–18]. With the measurements reported by the Belle and LHCb

collaborations [19–25], however, the deviations between the measured $R(D)$ and $R(D^*)$ and the SM predictions become smaller [26–29]:

(1) The latest Belle measurements [24] exhibit an excellent consistency with the averaged SM predictions [3–5, 29]:

$$R(D) = \begin{cases} 0.307 \pm 0.037(\text{stat.}) \pm 0.016(\text{syst.}), & \text{Belle}[24] \\ 0.299 \pm 0.003, & \text{SM}[29] \end{cases}, \tag{1}$$

$$R(D^*) = \begin{cases} 0.283 \pm 0.018(\text{stat.}) \pm 0.014(\text{syst.}), & \text{Belle}[24] \\ 0.258 \pm 0.005, & \text{SM}[29] \end{cases}, \tag{2}$$

since they are compatible within one standard deviation [24, 29].

(2) The combined analysis of currently available measurements of $R(D)$ and $R(D^*)$, including the new Belle results [24], gives the following world averaged values:

---

1) E-mail: hu-xueqing@qq.com
2) E-mail: 2223919088@qq.com
3) E-mail: xiaozhenjun@njnu.edu.cn

$$R(D)^{\text{Exp}} = 0.340 \pm 0.027 \pm 0.013,$$
$$R(D^*)^{\text{Exp}} = 0.295 \pm 0.011 \pm 0.008, \qquad (3)$$

so that the discrepancy decreases from the previous 3.8σ to 3.1σ with respect to the SM expectations [26, 27, 29].

(3) Besides the ratios $R(D^{(*)})$, other physical observables, such as the longitudinal polarization of the tau lepton $P_\tau(D^*)$ and the fraction of the D^* longitudinal polarization $F_L(D^*)$, were measured recently by the Belle collaboration [20, 21, 30]:

$$P_\tau(D^*) = -0.38 \pm 0.51(\text{stat.})^{+0.21}_{-0.16}(\text{syst.})[20, 21], \qquad (4)$$

$$F_L(D^*) = 0.60 \pm 0.08(\text{stat.}) \pm 0.04(\text{syst.})[30]. \qquad (5)$$

They are compatible with the SM predictions $P_\tau(D^*) = -0.497 \pm 0.013$ [31], $F_L(D^*) = 0.441(6)$ [32] and 0.457(10) [33] for the $B \to D^* \tau \bar\nu_\tau$ decays.

It is clear from the above points that although the anomalies of $R(D^{(*)})$ have become less serious recently, there is still a sizeable discrepancy with respect to the SM expectations, and that they should be investigated with complementary and more precise measurements in order to draw a conclusion. In addition to the $B \to D^{(*)} l \nu_l$ decays, the $B_s \to D_s^{(*)} l \nu_l$ decay mode is one of the best choices for cross examination. Systematic theoretical studies and experimental measurements of the semileptonic decays of B_s meson are therefore very important and should be performed promptly.

As illustrated by the Feynman diagrams in Fig. 1, the $B_{(s)} \to D_s^{(*)} l^+ \nu_l$ decays are closely related to the $B \to D^{(*)} l^+ \nu_l$ decays via the $SU(3)$ flavor symmetry. They are all controlled by the same $b \to c l \nu$ transitions at the quark level, but with a different spectator quark: (u,d) or s quark. As a consequence, in the limit of the $SU(3)$ flavor symmetry, these two sets of semileptonic decays must have very similar properties. If the current anomalies in $B \to D^{(*)} l \nu_l$ decays are indeed induced by contributions from NP, they must appear in the $B_s \to D_s^{(*)} l \nu_l$ decays. It is therefore necessary and very interesting to study the $B_s \to D_s^{(*)} l \nu_l$ decays and to measure the corresponding ratios $R(D_s^{(*)})$ and other relevant physical observables, such as $P_\tau(D_s^{(*)})$, $F_L(D_s^*)$ and $A_{FB}(\tau)$, in order to check if similar deviations exist.
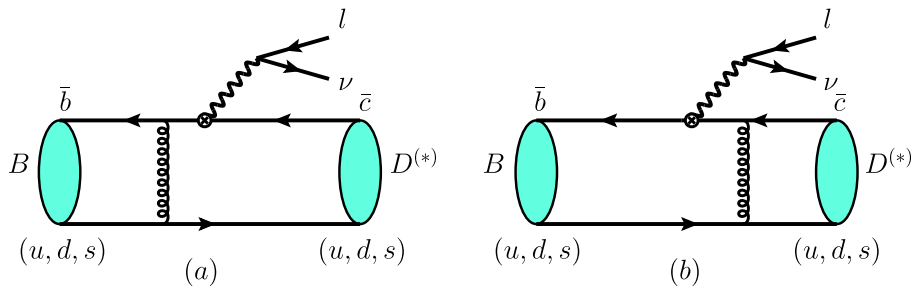
As is well known, the central issue for calculating such semileptonic decays in the SM framework is the estimate of the values and shapes of the form factors $(F_{+,0}(q^2), V(q^2), A_{0,1,2}(q^2))$ for the $B_{(s)} \to D_{(s)}^{(*)}$ transitions. However, calculations of these form factors are not easy and they cannot be estimated reliably in the whole range of momenta q^2 carried by the lepton pair using a single method, and their extrapolation is indispensable. There are many traditional methods and approaches to estimate the form factors and provide predictions of the ratios $R_{D^{(*)}}$, for example, the heavy quark effective theory (HQET) [4, 5], light cone sum rules (LCSR) [34–36], lattice QCD (LQCD) [37–41] and the perturbative QCD factorization approach (PQCD) [9, 10].

In recent years, the PQCD factorization approach has been used to study various kinds of semileptonic decays of $B/B_s/B_c$ mesons, as given for example in Refs. [9, 10, 42–48]. However, like in many other theoretical approaches, the form factors evaluated using the PQCD approach are only reliable in the low q^2 region. Therefore, extrapolations must be done in order to cover the whole range of q^2 values of the form factors $f_i(q^2)$. In order to improve the reliability of the values and shapes of the six form factors obtained in the PQCD approach, we include the lattice QCD result at the end point q^2_{max} so that the extrapolation from the low q^2 region to the high q^2 region is more reliable.

In Refs. [9, 10], the $B \to D^{(*)} l \nu_l$ decays were studied by employing the PQCD approach only [9], or with the inclusion of the lattice QCD input [10]. In Ref. [42], the $\bar{B}_s^0 \to D_s^{(*)} l^- \bar\nu_l$ decays were studied by employing the PQCD approach without the lattice QCD input. In this paper, we study the semileptonic decays of B and B_s mesons simultaneously and focus on the following three tasks:

(1) For the $B_s \to D_s^{(*)}$ and $B \to D^{(*)}$ transitions, we evaluate the relevant form factors in the region $0 \leqslant q^2 \leqslant m_l^2$ using the PQCD factorization approach, and then include the lattice QCD result at the end point q^2_{max} in the fitting process and extrapolate the form factors in the entire momentum region by employing the Bourrely-Caprini-Lellouch (BCL) parametrization [49, 50] instead

Fig. 1. (color online) Leading order Feynman diagrams for the semileptonic decays $B_{(s)} \to D_{(s)} l^+ \nu_l$ with $l = (e, \mu, \tau)$ in the PQCD approach.

of the pole models used in Refs. [9, 10, 42].

(2) In addition to the calculations of the branching ratios and the ratios $R(D_s^{(*)})$ and $R(D^{(*)})$, we also calculate three physical observables (which were not considered in [9, 10, 42]) for the decays of B and B_s mesons: the longitudinal polarization of the tau lepton $P_\tau(D_{(s)}^{(*)})$, the fraction of $D_{(s)}^*$ longitudinal polarization $F_L(D_{(s)}^*)$, and the forward-backward asymmetry of the tau lepton $A_{FB}(\tau)$ in the ordinary PQCD approach and the "PQCD +Lattice" approach (i.e. the PQCD approach with the inclusion of the lattice QCD input for the form factors).

(3) We present our theoretical predictions, compare them with the available experimental measurements, or the theoretical predictions obtained using other different theories or models.

The paper is organized as follows: In Sec. 2, we briefly review the kinematics of the $B_s^0 \to D_s^{(*)} l^+ \nu_l$ decays. The calculations of the form factors for the $B_s^0 \to D_s^{(*)}$ transitions are then given. We use the lattice QCD result at $q_{\max}^2$ given by the HPQCD group [41] as input in our extrapolation. Explicit expressions for the differential decay rates and additional physical observables are also given in Sec. 2. In Sec. 3, we present the theoretical predictions of the other physical observables obtained using the PQCD approach, the "PQCD+Lattice" approach and some other models. A short summary is given in the final section.

2   Theoretical framework

2.1   Kinematics and the wave functions

In the PQCD approach, the tree-level Feynman diagrams for $B_{(s)} \to D_{(s)}^{(*)} l\nu$ decays[1] are shown in Fig. 1. We define the $B_{(s)}$ meson momentum as p_1, the $D_{(s)}/D_{(s)}^*$ meson momentum as p_2, and the polarization vectors $\epsilon_{L,T}$ in the $D_{(s)}^*$ at $B_{(s)}$ rest frames as in Ref. [51].

$$p_1 = \frac{m_{B_{(s)}}}{\sqrt{2}}(1,1,0_\perp), \quad p_2 = \frac{r \cdot m_{B_{(s)}}}{\sqrt{2}}(\eta^+, \eta^-, 0_\perp),$$

$$\epsilon_L = \frac{1}{\sqrt{2}}(\eta^+, -\eta^-, 0_\perp), \quad \epsilon_T = (0,0,1), \qquad (6)$$

while ϵ_L and ϵ_T denote the longitudinal and transverse polarization of (D^*, D_s^*) mesons, respectively. The parameter $\eta^\pm$ and r are defined as:

$$\eta^\pm = \eta \pm \sqrt{\eta^2 - 1}, \quad \eta = \frac{1}{2r}\left(1 + r^2 - \frac{q^2}{m_{B_{(s)}}^2}\right), \quad r = \frac{m_{D_{(s)}^{(*)}}}{m_{B_{(s)}}}, \ (7)$$

where $q = p_1 - p_2$ is the momentum of the lepton pair. The momenta of the spectator quarks in $B_{(s)}$ and $D_{(s)}^{(*)}$ mesons are parametrized as

$$k_1 = \frac{m_{B_{(s)}}}{\sqrt{2}}(0, x_1, k_{1\perp}), \quad k_2 = \frac{r \cdot m_{B_{(s)}}}{\sqrt{2}}(x_2\eta^+, x_2\eta^-, k_{2\perp}), \quad (8)$$

where x_1 and x_2 are the fraction of the momentum carried by the light spectator quark in the initial B/B_s meson and the final state meson $D^{(*)}/D_{(s)}^{(*)}$, respectively.

For the B/B_s meson wave functions, we use the functions from Refs. [51, 52].

$$\Phi_{B_{(s)}}(x,b) = \frac{i}{\sqrt{2N_c}}(\not p_{B_{(s)}} + m_{B_{(s)}})\gamma_5 \phi_{B_{(s)}}(x,b), \qquad (9)$$

$$\phi_{B_{(s)}}(x,b) = N_{B_{(s)}} \cdot x^2(1-x)^2 \cdot \exp\left[-\frac{x^2 \cdot M_{B_{(s)}}^2}{2\omega_{B_{(s)}}^2} - \frac{1}{2}(\omega_{B_{(s)}} \cdot b)^2\right].$$

(10)

The normalization factor $N_{B_{(s)}}$ depends on the values of the parameter $\omega_{B_{(s)}}$ and decay constant $f_{B_{(s)}}$ through the normalization relation: $\int_0^1 dx\, \phi_{B_{(s)}}(x, b=0) = f_{B_{(s)}}/(2\sqrt{6})$. In order to estimate the uncertainties of theoretical predictions, we set the shape parameter $\omega_B = 0.40 \pm 0.04$ GeV and $\omega_{B_s} = 0.50 \pm 0.05$ GeV.

For $D_{(s)}$ and $D_{(s)}^*$ mesons, we use the same wave functions as in Ref. [53]

$$\Phi_{D_{(s)}}(p,x) = \frac{i}{\sqrt{6}}\gamma_5(\not p_{D_{(s)}} + m_{D_{(s)}})\phi_{D_{(s)}}(x), \qquad (11)$$

$$\Phi_{D_{(s)}^*}(p,x) = \frac{-i}{\sqrt{6}}\Big[\not\epsilon_L(\not p_{D_{(s)}^*} + m_{D_{(s)}^*})\phi_{D_{(s)}^*}^L(x)$$
$$+\not\epsilon_T(\not p_{D_{(s)}^*} + m_{D_{(s)}^*})\phi_{D_{(s)}^*}^T(x)\Big], \qquad (12)$$

with the distribution amplitudes

$$\phi_{D_{(s)}^{(*)}}(x) = \frac{f_{D_{(s)}^{(*)}}}{2\sqrt{6}} \cdot 6x(1-x)\Big[1 + C_{D_{(s)}^{(*)}}(1-2x)\Big]$$
$$\times \exp\left[-\frac{\omega^2 b^2}{2}\right], \qquad (13)$$

where we set the parameters $C_D = C_{D^*} = C_{D_s} = C_{D_s^*} = 0.5$ and $\omega = 0.1$. From the heavy quark limit, we assume that

$$f_{D^*}^L = f_{D^*}^T = f_{D^*}, \quad f_{D_s^*}^L = f_{D_s^*}^T = f_{D_s^*}, \qquad (14)$$

$$\phi_{D^*}^L = \phi_{D^*}^T = \phi_{D^*}, \quad \phi_{D_s^*}^L = \phi_{D_s^*}^T = \phi_{D_s^*}. \qquad (15)$$

2.2   Form factors in the PQCD approach

The form factors of the $B_{(s)} \to D_{(s)}$ transition are defined in the same form as in Ref. [54]

$$\langle D_{(s)}(p_2)|\bar c(0)\gamma_\mu b(0)|B_{(s)}(p_1)\rangle = \left[(p_1+p_2)_\mu - \frac{m_{B_{(s)}}^2 - m_{D_{(s)}}^2}{q^2}q_\mu\right]$$

$$\times F_+(q^2) + \left[\frac{m_{B_{(s)}}^2 - m_{D_{(s)}}^2}{q^2}q_\mu\right]F_0(q^2). \qquad (16)$$

In order to cancel the poles at $q^2 = 0$, $F_+(0)$ should be

---

1) Throughout this paper the symbol $B_{(s)}$ describes both $B=(B_u, B_d)$ and B_s mesons.

equal to $F_0(0)$. For convenience, we also define the auxiliary form factors $f_1(q^2)$ and $f_2(q^2)$,

$$\langle D_{(s)}(p_2)|\bar{c}(0)\gamma_\mu b(0)|B_{(s)}(p_1)\rangle = f_1(q^2)p_{1\mu} + f_2(q^2)p_{2\mu}, \quad (17)$$

which are related to $F_+(q^2)$ and $F_0(q^2)$ by the following relations,

$$F_+(q^2) = \frac{1}{2}\left[f_1(q^2) + f_2(q^2)\right], \quad (18)$$

$$F_0(q^2) = \frac{1}{2}f_1(q^2)\left[1 + \frac{q^2}{m_{B_{(s)}}^2 - m_{D_{(s)}}^2}\right]$$
$$+ \frac{1}{2}f_2(q^2)\left[1 - \frac{q^2}{m_{B_{(s)}}^2 - m_{D_{(s)}}^2}\right]. \quad (19)$$

For vector meson $D_{(s)}^*$ in the final state, the form factors for $B_{(s)} \to D_{(s)}^*$ transitions are $V(q^2)$ and $A_{0,1,2}(q^2)$, which are given in the following form [54] :

$$\langle D_{(s)}^*(p_2)|\bar{c}(0)\gamma_\mu b(0)|B_{(s)}(p_1)\rangle = \frac{2iV(q^2)}{m_{B_{(s)}} + m_{D_{(s)}^*}}\epsilon_{\mu\nu\alpha\beta}\epsilon^{*\nu}p_1^\alpha p_2^\beta, \quad (20)$$

$$\langle D_{(s)}^*(p_2)|\bar{c}(0)\gamma_\mu\gamma_5 b(0)|B_{(s)}(p_1)\rangle = 2m_{D_{(s)}^*}A_0(q^2)\frac{\epsilon^*\cdot q}{q^2}q_\mu + (m_{B_{(s)}} + m_{D_{(s)}^*})A_1(q^2)\left(\epsilon_\mu^* - \frac{\epsilon^*\cdot q}{q^2}q_\mu\right)$$
$$- A_2(q^2)\frac{\epsilon^*\cdot q}{m_{B_{(s)}} + m_{D_{(s)}^*}}\left[(p_1 + p_2)_\mu - \frac{m_{B_{(s)}}^2 - m_{D_{(s)}^*}^2}{q^2}q_\mu\right]. \quad (21)$$

The analytical expressions for the form factors mentioned above are the following:

$$f_1(q^2) = 8\pi m_{B_{(s)}}^2 C_F \int dx_1 dx_2 \int b_1 db_1 b_2 db_2 \phi_{B_{(s)}}(x_1, b_1)\phi_{D_{(s)}}(x_2, b_2)\bigg\{[2r(1 - rx_2)]\cdot H_1(t_1)$$
$$+ \left[2r(2r_c - r) + x_1 r\left(-2 + 2\eta + \sqrt{\eta^2 - 1} - \frac{2\eta}{\sqrt{\eta^2 - 1}} + \frac{\eta^2}{\sqrt{\eta^2 - 1}}\right)\right]\cdot H_2(t_2)\bigg\}, \quad (22)$$

$$f_2(q^2) = 8\pi m_{B_{(s)}}^2 C_F \int dx_1 dx_2 \int b_1 db_1 b_2 db_2 \phi_{B_{(s)}}(x_1, b_1)\phi_{D_{(s)}}(x_2, b_2)$$
$$\times \bigg\{[2 - 4x_2 r(1 - \eta)]\cdot H_1(t_1) + \left[4r - 2r_c - x_1 + \frac{x_1}{\sqrt{\eta^2 - 1}}(2 - \eta)\right]\cdot H_2(t_2)\bigg\}, \quad (23)$$

where the mass ratios are $r_c = m_c/m_{B_{(s)}}$, $r = m_{D_{(s)}}/m_{B_{(s)}}$.

$$V(q^2) = 8\pi m_{B_{(s)}}^2 C_F \int dx_1 dx_2 \int b_1 db_1 b_2 db_2 \phi_{B_{(s)}}(x_1, b_1)\phi_{D_{(s)}^*}^T(x_2, b_2)\cdot(1 + r)\bigg\{[1 - rx_2]\cdot H_1(t_1) + \left[r + \frac{x_1}{2\sqrt{\eta^2 - 1}}\right]\cdot H_2(t_2)\bigg\}, \quad (24)$$

$$A_0(q^2) = 8\pi m_{B_{(s)}}^2 C_F \int dx_1 dx_2 \int b_1 db_1 b_2 db_2 \phi_{B_{(s)}}(x_1, b_1)\phi_{D_{(s)}^*}^L(x_2, b_2)\bigg\{[1 + r - rx_2(2 + r - 2\eta)]\cdot H_1(t_1)$$
$$+ \left[r^2 + r_c + \frac{x_1}{2} + \frac{\eta x_1}{2\sqrt{\eta^2 - 1}} + \frac{rx_1}{2\sqrt{\eta^2 - 1}}\left(1 - 2\eta\left(\eta + \sqrt{\eta^2 - 1}\right)\right)\right]\cdot H_2(t_2)\bigg\}, \quad (25)$$

$$A_1(q^2) = 8\pi m_{B_{(s)}}^2 C_F \int dx_1 dx_2 \int b_1 db_1 b_2 db_2 \phi_{B_{(s)}}(x_1, b_1)\phi_{D_{(s)}^*}^T(x_2, b_2)\cdot\frac{r}{1 + r}$$
$$\times \bigg\{2[1 + \eta - 2rx_2 + r\eta x_2]\cdot H_1(t_1) + [2r_c + 2\eta r - x_1]\cdot H_2(t_2)\bigg\}, \quad (26)$$

$$A_2(q^2) = \frac{(1 + r)^2(\eta - r)}{2r(\eta^2 - 1)}\cdot A_1(q^2) - 8\pi m_{B_{(s)}}^2 C_F \int dx_1 dx_2 \int b_1 db_1 b_2 db_2 \phi_{B_{(s)}}(x_1, b_1)\cdot\phi_{D_{(s)}^*}^L(x_2, b_2)\cdot\frac{1 + r}{\eta^2 - 1}$$
$$\times \bigg\{[(1 + \eta)(1 - r) - rx_2(1 - 2r + \eta(2 + r - 2\eta))]\cdot H_1(t_1)$$
$$+ \left[r + r_c(\eta - r) - \eta r^2 + rx_1\eta^2 - \frac{x_1}{2}(\eta + r) + x_1\left(\eta r - \frac{1}{2}\right)\sqrt{\eta^2 - 1}\right]\cdot H_2(t_2)\bigg\}, \quad (27)$$

where the color factor is $C_F = 4/3$, the mass ratios are $r_c = m_c/m_{B_{(s)}}$, $r = m_{D^*_{(s)}}/m_{B_{(s)}}$ and the functions $H_i(t_i)$ are in the following form

$$H_i(t_i) = h_i(x_1, x_2, b_1, b_2) \cdot \alpha_s(t_i) \exp\left[-S_{ab}(t_i)\right], \text{ for } i = (1, 2).$$
(28)

The explicit expressions for the hard functions $h_i(x_1, x_2, b_1, b_2)$, hard scales t_i and the Sudakov factors $[-S_{ab}(t_i)]$ are given in the Appendix.

2.3 Lattice input at q^2_{max}

The lattice QCD has advantages in calculating the form factors for large q^2, and it is generally believed that the lattice QCD predictions close to or at q^2_{max} are reliable. In this work, we make use of the lattice QCD predictions of all relevant form factors at the endpoint q^2_{max} as the additional input in the fitting process, so as to make the extrapolation of these form factors from the low q^2 region to q^2_{max} more reliable.

The form factors used in the lattice QCD are parametrized as follows [55, 56]:

$$\langle D_{(s)}|\bar{c}V^\mu b|B_{(s)}\rangle = \sqrt{m_{B_{(s)}}m_{D_{(s)}}}\left[h_+(w)(\upsilon+\upsilon')^\mu + h_-(w)(\upsilon-\upsilon')^\mu\right],$$

$$\langle D^*_{(s)}|\bar{c}V^\mu b|B_{(s)}\rangle = \sqrt{m_{B_{(s)}}m_{D^*_{(s)}}}i\varepsilon^{\mu\nu}_{\rho\sigma}\epsilon^*_\nu \upsilon^\rho \upsilon'^\sigma h_V(w),$$

$$\langle D^*_{(s)}|\bar{c}A^\mu b|B_{(s)}\rangle = \sqrt{m_{B_{(s)}}m_{D^*_{(s)}}}\epsilon^*_\nu \left[g^{\mu\nu}(1+w)h_{A_1}(w)\right.$$
$$\left.-\upsilon^\nu(\upsilon^\mu h_{A_2}(w) + \upsilon'^\mu h_{A_3}(w))\right],$$
(29)

where $\upsilon = p_{B_{(s)}}/m_{B_{(s)}}$, $\upsilon' = p_{D^*_{(s)}}/m_{D^*_{(s)}}$, the velocity transfer is $w = \upsilon \cdot \upsilon'$, and ϵ is the polarization vector of the $D^*_{(s)}$ meson. With a simple transformation, we can relate them to the form factors used in our work:

$$F_+(q^2) = \frac{1}{2\sqrt{r}}\left[(1+r)h_+(w) - (1-r)h_-(w)\right],$$

$$F_0(q^2) = \sqrt{r}\left[\frac{1+w}{1+r}h_+(w) - \frac{w-1}{1-r}h_-(w)\right],$$
(30)

where $w = (m^2_{B_{(s)}} + m^2_{D_{(s)}} - q^2)/(2m_{B_{(s)}}m_{D_{(s)}})$, and

$$V(q^2) = \frac{1+r}{2\sqrt{r}}h_V(w),$$

$$A_0(q^2) = \frac{1}{2\sqrt{r}}\left[(1+w)h_{A_1}(w) - (1-wr)h_{A_2}(w) + (r-w)h_{A_3}(w)\right],$$

$$A_1(q^2) = \frac{\sqrt{r}}{1+r}(1+w)h_{A_1}(w),$$

$$A_2(q^2) = \frac{1+r}{2\sqrt{r}}(rh_{A_2}(w) + h_{A_3}(w)),$$
(31)

where $w = (m^2_{B_{(s)}} + m^2_{D^*_{(s)}} - q^2)/(2m_{B_{(s)}}m_{D^*_{(s)}})$.

At the end point $q^2 = q^2_{max}$, we have

$$h_V(1) = h_{A_1}(1) = h_{A_3}(1), \quad h_{A_2}(1) = 0, \quad h_{A_1}(1) = \mathcal{F}(1),$$

$$w = 1, \quad \left[h_+(1) - \frac{(1-r)}{(1+r)}h_-(1)\right] = \mathcal{G}(1).$$
(32)

Therefore, the relevant form factors at the endpoint q^2_{max}

become:

$$F_+(q^2_{max}) = \frac{1+r}{2\sqrt{r}}\mathcal{G}(1),$$

$$V(q^2_{max}) = A_0(q^2_{max}) = A_2(q^2_{max}) = \frac{1}{A_1(q^2_{max})} = \frac{1+r}{2\sqrt{r}}\mathcal{F}(1).$$
(33)

Using the formulas above and including the lattice input [41, 57]

$$\mathcal{G}^{B\to D}(1) = 1.033 \pm 0.095,$$
$$\mathcal{F}^{B\to D^*}(1) = 0.895 \pm 0.010 \pm 0.024,$$
$$\mathcal{G}^{B_s\to D_s}(1) = 1.052 \pm 0.046,$$
$$\mathcal{F}^{B_s\to D^*_s}(1) = 0.883 \pm 0.012 \pm 0.028,$$
(34)

with the relation between F_0 and F_+ near the endpoint q^2_{max} evaluated in Ref. [57]:

$$F_0^{B\to D}/F_+^{B\to D} = 0.73 \pm 0.04,$$
$$F_0^{B_s\to D_s}/F_+^{B_s\to D_s} = 0.77 \pm 0.02,$$
(35)

we find the following values of the relevant form factors at the endpoint q^2_{max}:

$$F_0^{B\to D}(q^2_{max}) = 0.86 \pm 0.08, \quad F_0^{B_s\to D_s}(q^2_{max}) = 0.91 \pm 0.05,$$
$$F_+^{B\to D}(q^2_{max}) = 1.17 \pm 0.10, \quad F_+^{B_s\to D_s}(q^2_{max}) = 1.19 \pm 0.05,$$
$$V^{B\to D^*}(q^2_{max}) = 1.01 \pm 0.05, \quad V^{B_s\to D^*_s}(q^2_{max}) = 0.98 \pm 0.05,$$
$$A_0^{B\to D^*}(q^2_{max}) = 1.01 \pm 0.05, \quad A_0^{B_s\to D^*_s}(q^2_{max}) = 0.98 \pm 0.05,$$
$$A_1^{B\to D^*}(q^2_{max}) = 0.80 \pm 0.04, \quad A_1^{B_s\to D^*_s}(q^2_{max}) = 0.79 \pm 0.04,$$
$$A_2^{B\to D^*}(q^2_{max}) = 1.01 \pm 0.05, \quad A_2^{B_s\to D^*_s}(q^2_{max}) = 0.98 \pm 0.05.$$
(36)

The uncertainty of the form factors comes from the errors of $\mathcal{G}(1)$, given in Eq. (34), is around $5\% \sim 10\%$, while the uncertainty of $\mathcal{F}(1)$ is around 2%. We set conservatively a common error of 5% for the form factors $V, A_{0,1,2}$ in Eq. (36), which takes into account the small variations of the central values of $\mathcal{G}(1)$ and $\mathcal{F}(1)$ in recent years [41, 55–57].

2.4 Extrapolation and differential decay rates

We know that the form factors calculated in the PQCD approach are only reliable in the low q^2 region. In order to cover the whole momentum range $m_l^2 \leqslant q^2 \leqslant q^2_{max}$ we have to perform an extrapolation. In order to improve the reliability of the extrapolation, we also use the values of the form factors at the endpoint q^2_{max} evaluated in lattice QCD.

In the previous works [9, 42], we used the pole model parametrization [58] to perform the fit. In this work, we use the Bourrely-Caprini-Lellouch (BCL) parametrization [49] instead, and match it to the lattice input to improve the reliability of the extrapolation. We use our PQCD predictions of the form factors $f_i(q^2)$ at sixteen points in the interval $0 \leqslant q^2 \leqslant m_\tau^2$, and the lattice QCD

value as an additional input at the endpoint q^2_{max}. Analogous to Ref. [50], we consider only the first two terms of the series in parameter z:

$$
\begin{aligned}
f_i(t) &= \frac{1}{1 - t/m_R^2} \sum_{k=0}^{1} \alpha_k^i z^k(t, t_0) \\
&= \frac{1}{1 - t/m_R^2} \left(\alpha_0^i + \alpha_1^i \frac{\sqrt{t_+ - t} - \sqrt{t_+ - t_0}}{\sqrt{t_+ - t} + \sqrt{t_+ - t_0}} \right),
\end{aligned}
\tag{37}
$$

with

$$
0 \leqslant t_0 = t_+ \left(1 - \sqrt{1 - \frac{t_-}{t_+}} \right) \leqslant t_-,
\tag{38}
$$

where $t = q^2$, $t_\pm = (m_{B_{(s)}} \pm m_{D_{(s)}^{(*)}})^2$, and m_R are the masses of the low-lying resonances. The optimized value of t_0 is chosen to be the same as in Ref. [50]. Since the choice of m_R depends on the charged currents of semileptonic decays, i.e. of the $b \to c l \bar{\nu}_l$ or the $b \to u l \bar{\nu}_l$ transitions, we use the same set of m_R as in Ref. [50], where the $B_c \to (\eta_c, J/\psi) l \bar{\nu}_l$ decays have the same quark level $b \to c l \bar{\nu}_l$ transitions as in this paper.

With these extrapolations, we have access to the full momentum dependence of the form factors, and the branching ratios of the semileptonic decays $B_{(s)} \to D_{(s)}^{(*)} l \nu$ can be calculated. The quark level transition in these semileptonic decays is $b \to c l \nu$ with the effective Hamiltonian [59]

$$
\mathcal{H}_{\text{eff}}(b \to c l \nu) = \frac{G_F}{\sqrt{2}} V_{cb} \, \bar{c} \gamma_\mu (1 - \gamma_5) b \cdot \bar{l} \gamma^\mu (1 - \gamma_5) \nu_l,
\tag{39}
$$

where $G_F = 1.16637 \times 10^{-5} \text{GeV}^{-2}$ is the Fermi constant. The differential decay rates of the decay mode $B_{(s)} \to D_{(s)} l \nu$ can be expressed as [60]:

$$
\begin{aligned}
\frac{\mathrm{d}\Gamma(B_{(s)} \to D_{(s)} l \nu)}{\mathrm{d}q^2} &= \frac{G_F^2 |V_{cb}|^2}{192 \pi^3 m_{B_{(s)}}^3} \left(1 - \frac{m_l^2}{q^2} \right)^2 \frac{\lambda^{1/2}(q^2)}{2q^2} \\
&\times \left\{ 3 m_l^2 \left(m_{B_{(s)}}^2 - m_{D_{(s)}}^2 \right)^2 |F_0(q^2)|^2 \right. \\
&\left. + \left(m_l^2 + 2q^2 \right) \lambda(q^2) |F_+(q^2)|^2 \right\},
\end{aligned}
\tag{40}
$$

where m_l is the mass of leptons e, μ or τ, and $\lambda(q^2) = (m_{B_{(s)}}^2 + m_{D_{(s)}}^2 - q^2)^2 - 4 m_{B_{(s)}}^2 m_{D_{(s)}}^2$ is the phase space factor.

For the decay mode $B_{(s)} \to D_{(s)}^* l \nu$, the differential decay widths can be written as [58]:

$$
\begin{aligned}
\frac{\mathrm{d}\Gamma_L(B_{(s)} \to D_{(s)}^* l \nu)}{\mathrm{d}q^2} &= \frac{G_F^2 |V_{cb}|^2}{192 \pi^3 m_{B_{(s)}}^3} \left(1 - \frac{m_l^2}{q^2} \right)^2 \frac{\lambda^{1/2}(q^2)}{2q^2} \cdot \left\{ 3 m_l^2 \lambda(q^2) A_0^2(q^2) \right. \\
&\left. + \frac{m_l^2 + 2q^2}{4 m_{D_{(s)}^*}^2} \left[\left(m_{B_{(s)}}^2 - m_{D_{(s)}^*}^2 - q^2 \right) \left(m_{B_{(s)}} + m_{D_{(s)}^*} \right) A_1(q^2) - \frac{\lambda(q^2) A_2(q^2)}{m_{B_{(s)}} + m_{D_{(s)}^*}} \right]^2 \right\},
\end{aligned}
\tag{41}
$$

$$
\frac{\mathrm{d}\Gamma_T(B_{(s)} \to D_{(s)}^* l \nu)}{\mathrm{d}q^2} = \frac{G_F^2 |V_{cb}|^2}{192 \pi^3 m_{B_{(s)}}^3} \left(1 - \frac{m_l^2}{q^2} \right)^2 \lambda^{3/2}(q^2) \left(m_l^2 + 2q^2 \right) \left[\frac{V^2(q^2)}{\left(m_{B_{(s)}} + m_{D_{(s)}^*} \right)^2} + \frac{\left(m_{B_{(s)}} + m_{D_{(s)}^*} \right)^2 A_1^2(q^2)}{\lambda(q^2)} \right],
\tag{42}
$$

with the phase space factor $\lambda(q^2) = (m_{B_{(s)}}^2 + m_{D_{(s)}^*}^2 - q^2)^2 - 4 m_{B_{(s)}}^2 m_{D_{(s)}^*}^2$. The total differential decay width is defined as:

$$
\frac{\mathrm{d}\Gamma}{\mathrm{d}q^2} = \frac{\mathrm{d}\Gamma_L}{\mathrm{d}q^2} + \frac{\mathrm{d}\Gamma_T}{\mathrm{d}q^2}.
\tag{43}
$$

2.5 Additional physical observables P_τ, $F_L(D_{(s)}^*)$ and $A_{FB}(\tau)$

Besides the decay rates and the ratios $R(X)$, there are three additional physical observables for the B/B_s semileptonic decays: the longitudinal polarization of the tau lepton P_τ, the fraction of $D_{(s)}^*$ longitudinal polarization $F_L(D_{(s)}^*)$ and the forward-backward asymmetry of the tau lepton $A_{FB}(\tau)$. These physical observables are sensitive to new physics beyond SM [2, 61, 62].

As for the definitions of these physical observables, we follow Refs. [31, 63, 64]. For the τ longitudinal polarization, for example, the authors of Refs. [31, 63] used the Q rest frame, where the spatial components of the momentum transfer $Q = p_B - p_M$ vanish. In this coordinate system the direction of the B momenta is along the z axis, and the τ momentum lies in the $x - z$ plane. Here, we use the same definition:

$$
P_\tau(D_{(s)}^{(*)}) = \frac{\Gamma_+(D_{(s)}^{(*)}) - \Gamma_-(D_{(s)}^{(*)})}{\Gamma_+(D_{(s)}^{(*)}) + \Gamma_-(D_{(s)}^{(*)})},
\tag{44}
$$

where $\Gamma_\pm(D_{(s)}^{(*)})$ denotes the decay rate of $B_{(s)} \to D_{(s)}^{(*)} \tau \bar{\nu}_\tau$ with the τ lepton helicity of $\pm 1/2$. The explicit expressions for $\Gamma_\pm$ in SM can be found in the Appendix of Ref. [64]. For $B_{(s)} \to D_{(s)} \tau \bar{\nu}_\tau$ decays, we find

$$
\frac{\mathrm{d}\Gamma_+}{\mathrm{d}q^2} = \frac{G_F^2 |V_{cb}|^2}{192 \pi^3 m_{B_{(s)}}^3} q^2 \sqrt{\lambda(q^2)} \left(1 - \frac{m_\tau^2}{q^2} \right)^2 \frac{m_\tau^2}{2q^2} \left(H_{V,0}^{s\,2} + 3 H_{V,t}^{s\,2} \right),
\tag{45}
$$

$$
\frac{\mathrm{d}\Gamma_-}{\mathrm{d}q^2} = \frac{G_F^2 |V_{cb}|^2}{192 \pi^3 m_{B_{(s)}}^3} q^2 \sqrt{\lambda(q^2)} \left(1 - \frac{m_\tau^2}{q^2} \right)^2 \left(H_{V,0}^{s\,2} \right).
\tag{46}
$$

For $B_{(s)} \to D_{(s)}^* \tau \bar{\nu}_\tau$ decays, we have

$$\frac{d\Gamma_+}{dq^2} = \frac{G_F^2 |V_{cb}|^2}{192\pi^3 m_{B_{(s)}}^3} q^2 \sqrt{\lambda(q^2)} \left(1 - \frac{m_\tau^2}{q^2}\right)^2 \frac{m_\tau^2}{2q^2}$$
$$\times \left(H_{V,+}^2 + H_{V,-}^2 + H_{V,0}^2 + 3H_{V,t}^2\right), \qquad (47)$$

$$\frac{d\Gamma_-}{dq^2} = \frac{G_F^2 |V_{cb}|^2}{192\pi^3 m_{B_{(s)}}^3} q^2 \sqrt{\lambda(q^2)} \left(1 - \frac{m_\tau^2}{q^2}\right)^2 \left(H_{V,+}^2 + H_{V,-}^2 + H_{V,0}^2\right), \qquad (48)$$

where the functions $(H_{V,0}^s, H_{V,t}^s, H_{V,\pm}, H_{V,0}, H_{V,t})$ can be written as combinations of the six form factors defined in Eqs. (18), (19), (22)-(27):

$$H_{V,0}^s(q^2) = \sqrt{\frac{\lambda(q^2)}{q^2}} F_+(q^2), \qquad (49)$$

$$H_{V,t}^s(q^2) = \frac{m_{B_{(s)}}^2 - m_{D_{(s)}}^2}{\sqrt{q^2}} F_0(q^2), \qquad (50)$$

$$H_{V,\pm}(q^2) = (m_{B_{(s)}} + m_{D_{(s)}^*})A_1(q^2) \mp \frac{\sqrt{\lambda(q^2)}}{m_{B_{(s)}} + m_{D_{(s)}^*}} V(q^2), \quad (51)$$

$$H_{V,0}(q^2) = \frac{m_{B_{(s)}} + m_{D_{(s)}^*}}{2m_{D_{(s)}^*} \sqrt{q^2}} \left[-(m_{B_{(s)}}^2 - m_{D_{(s)}^*}^2 - q^2)A_1(q^2) \right.$$
$$\left. + \frac{\lambda(q^2)A_2(q^2)}{(m_{B_{(s)}} + m_{D_{(s)}^*})^2} \right], \qquad (52)$$

$$H_{V,t}(q^2) = -\sqrt{\frac{\lambda(q^2)}{q^2}} A_0(q^2). \qquad (53)$$

The phase space factor λ is the same as in Eqs. (40)-(42).

The fraction of $D_{(s)}^*$ longitudinal polarization $F_L(D_{(s)}^*)$ is defined using the secondary decay chain $D_{(s)}^* \to D_{(s)}\pi$ of the semileptonic B/B_s decays. It is given in the form [64]:

$$F_L(D_{(s)}^*) = \frac{\Gamma^0}{\Gamma^0 + \Gamma^{+1} + \Gamma^{-1}}, \qquad (54)$$

and the corresponding differential decay rates have the following form:

$$\frac{d\Gamma^{\pm 1}}{dq^2} = \frac{G_F^2 |V_{cb}|^2}{192\pi^3 m_{B_{(s)}}^3} q^2 \sqrt{\lambda(q^2)} \left(1 - \frac{m_\tau^2}{q^2}\right)^2 \left(1 + \frac{m_\tau^2}{2q^2}\right)(H_{V,\pm}^2), \qquad (55)$$

$$\frac{d\Gamma^0}{dq^2} = \frac{G_F^2 |V_{cb}|^2}{192\pi^3 m_{B_{(s)}}^3} q^2 \sqrt{\lambda(q^2)} \left(1 - \frac{m_\tau^2}{q^2}\right)^2$$
$$\times \left[\left(1 + \frac{m_\tau^2}{2q^2}\right)H_{V,0}^2 + \frac{3}{2}\frac{m_\tau^2}{q^2}H_{V,t}^2\right]. \qquad (56)$$

The τ lepton forward-backward asymmetry $A_{FB}(\tau)$ is more complicated since it is defined in the $\tau\bar{\nu}$ rest frame. The explicit expression is [64]:

$$A_{FB} = \frac{\int_0^1 \frac{d\Gamma}{d\cos\theta} d\cos\theta - \int_{-1}^0 \frac{d\Gamma}{d\cos\theta} d\cos\theta}{\int_{-1}^1 \frac{d\Gamma}{d\cos\theta} d\cos\theta} = \frac{\int b_\theta(q^2) dq^2}{\Gamma_{B_{(s)}}}, \qquad (57)$$

where θ is the angle between the 3-momenta of τ and the initial B or B_s in the $\tau\bar{\nu}$ rest frame. The function $b_\theta(q^2)$ is the angular coefficient which can be written as [64]:

$$b_\theta^{(D)}(q^2) = \frac{G_F^2 |V_{cb}|^2}{128\pi^3 m_{B_{(s)}}^3} q^2 \sqrt{\lambda(q^2)} \left(1 - \frac{m_\tau^2}{q^2}\right)^2 \frac{m_\tau^2}{q^2}(H_{V,0}^s H_{V,t}^s), \qquad (58)$$

$$b_\theta^{(D^*)}(q^2) = \frac{G_F^2 |V_{cb}|^2}{128\pi^3 m_{B_{(s)}}^3} q^2 \sqrt{\lambda(q^2)} \left(1 - \frac{m_\tau^2}{q^2}\right)^2$$
$$\left[\frac{1}{2}(H_{V,+}^2 - H_{V,-}^2) + \frac{m_\tau^2}{q^2}(H_{V,0}H_{V,t})\right]. \qquad (59)$$

With the above definitions and formulas, we are now ready to present our numerical results and a phenomenological analysis.

3   Numerical results and discussion

In the numerical calculations, we use the following parameters (masses and decay constants are in units of GeV) [28, 29, 65, 66]:

$$m_B = 5.28, \quad m_{B_s} = 5.367, \quad m_{D_0} = 1.865, \quad m_{D_+} = 1.870,$$
$$m_{D_0^*} = 2.007, \quad m_{D_+^*} = 2.010, \quad m_{D_s} = 1.968,$$
$$m_{D_s^*} = 2.112, \quad m_\tau = 1.777, \quad m_c = 1.275^{+0.025}_{-0.035},$$
$$f_D = 0.212, \quad f_{D_s} = 0.249, \quad f_{B_+} = 0.187, \quad f_{B_0} = 0.191,$$
$$f_{B_s} = 0.227, \quad |V_{cb}| = (42.2 \pm 0.8) \times 10^{-3}, \quad \tau_{B_+} = 1.638\text{ps},$$
$$\tau_{B_0} = 1.520\text{ps}, \quad \tau_{B_s} = 1.509\text{ps}, \quad f_{D^*} = (1.078 \pm 0.036) \cdot f_D,$$
$$f_{D_s^*} = (1.087 \pm 0.020) \cdot f_{D_s}, \quad \Lambda_{\overline{\text{MS}}}^{(f=4)} = 0.287. \qquad (60)$$

3.1   Form factors

It is obvious that the theoretical predictions of the differential decay rates and other physical observables for the considered semileptonic B/B_s meson decays strongly depend on the form factors $F_{0,+}(q^2)$, $V(q^2)$ and $A_{0,1,2}(q^2)$. Specifically, $F_{0,+}(q^2)$ controls the process $B_{(s)} \to D_{(s)}l\nu_l$, while $V(q^2)$ and $A_{0,1,2}(q^2)$ play key roles in the process $B_{(s)} \to D_{(s)}^*l\nu_l$. The value of these form factors at $q^2 = 0$ and their q^2 dependence in the range $0 \leqslant q^2 \leqslant q_{\text{max}}^2$ contain a lot of information about the relevant physical processes.

In Refs. [9, 51, 53], the applicability of the PQCD approach to $(B \to D^{(*)})$ transitions was examined, and it was shown that the PQCD approach with the inclusion of the Sudakov effects is applicable to the semileptonic decays

$B \to D^{(*)} l \bar{\nu}_l$ in the low q^2 region. Therefore, we present our predictions of the form factors at $q^2 = 0$ in Table 1.

It can be seen from Table 1 that the form factors for $B \to D^{(*)}$ and $B_s \to D_s^{(*)}$ transitions are very similar at $q^2 = 0$, which implies that the effect of $SU(3)$ flavor symmetry breaking is small, less than 10%. In order to cover the whole q^2 region, an extrapolation of the form factors has to be made from $q^2 = 0$ up to $q^2 = q^2_{max}$. In this work, we make the extrapolation using two different methods.

Table 1.   Theoretical predictions of the form factors at $q^2 = 0$ using the PQCD approach with BCL parametrization [49, 50].

	$F_{(0,+)}(0)$	$V(0)$	$A_0(0)$	$A_1(0)$	$A_2(0)$
$B^+ \to D^0$	0.53 ± 0.10	–	–	–	–
$B^0 \to D^-$	0.54 ± 0.10	–	–	–	–
$B_s^0 \to D_s^-$	0.52 ± 0.10	–	–	–	–
$B^+ \to D^{*0}$	–	0.64 ± 0.11	0.49 ± 0.08	0.51 ± 0.09	0.54 ± 0.09
$B^0 \to D^{*-}$	–	0.65 ± 0.11	0.50 ± 0.09	0.52 ± 0.08	0.55 ± 0.10
$B_s^0 \to D_s^{*-}$	–	0.64 ± 0.12	0.48 ± 0.09	0.50 ± 0.09	0.53 ± 0.11

(1) The first method is analogous to that used in Refs. [9, 42]. We first calculate the form factors at several points in the lower region $0 \leqslant q^2 \leqslant m_\tau^2$ using the expressions in Eqs. (22)-(27) and the definitions in Eqs. (18), (19). In the fitting process, we use the BCL parametrization formula given in Eqs. (37), (38) instead of the pole model parametrization used in Refs. [9, 42].

(2) The second method is the "PQCD+Lattice" method, similar to Ref. [10]. Since the lattice QCD results for the form factors are reliable and accurate at $q^2 \cong q^2_{max}$, we take the lattice QCD predictions of the form factors at the endpoint q^2_{max} as an additional input in the fitting process. In order to match the lattice input, we use the BCL parametrization [49, 50] for extrapolation.

In Figs. 2 and 3, we show the theoretical predictions of the q^2 dependence of the six form factors for $B^+ \to (D^0, D^{*0})$ and $B_s \to (D_s^-, D_s^{*-})$ transitions, obtained by employing the PQCD approach (blue solid curves) and the "PQCD + Lattice" method (red dashed curves). The blue and red bands show the theoretical uncertainties. As a comparison, we also show the central values of the PQCD predictions of the form factors (orange dashed curves) with the pole model parametrization [9, 42, 58]. One can see from the theoretical predictions listed in Table 1 and illustrated in Figs. 2 and 3 that:

(1) The form factors for $B \to D^{(*)}$ and $B_s \to D_s^{(*)}$ transitions have very similar values in the whole q^2 range due to the $SU(3)$ flavor symmetry.

(2) The differences between the theoretical predictions of the form factors in the traditional PQCD approach and the "PQCD+Lattice" method are small for low q^2 and remain moderate for large q^2, in particular for $F_{0,+}(q^2)$ and $A_{0,1,2}(q^2)$. For $V(q^2)$, the difference is more pronounced for large q^2. For the $B \to D^*$ transition, we found $V(10.71) \approx 1.53$ (1.06) in the PQCD approach ("PQCD + Lattice" method). For the $B_s \to D_s^*$ transition, we found a very similar result.

(3) The difference between the PQCD predictions of the central values of the form factors obtained using the traditional pole model and the BCL model is very small in the region $q^2 < 8$ GeV^2. The largest differences in the region near q^2_{max} are $\Delta F_+(11.55) = 0.59$ (i.e, about 31% of $F_+(11.55) = 1.89$ in the pole model), and $\Delta V(10.59) = 0.36$ (i.e. about 19% of $V(10.59) = 1.89$ in the pole model) for the $B_s \to D_s^{(*)}$ transition, as illustrated in Fig. 3.

3.2   Branching ratios and the ratio of Brs

Inserting the obtained form factors in the differential decay rates given in Eqs. (40)-(43), it is straightforward to integrate over the range $m_l^2 \leqslant q^2 \leqslant (m_{B_{(s)}} - m_{D_{(s)}^{(*)}})^2$. For the four semileptonic decays $B_s^0 \to D_s^{(*)} \tau^+ \nu_\tau$ and $B_s \to D_s^{(*)} l^+ \nu_l$ with $l^+ = (e^+, \mu^+)$, the theoretical predictions of the branching ratios are the following:

$$\mathcal{B}(B_s^0 \to D_s^- \tau^+ \nu_\tau) = \begin{cases} 0.72^{+0.32}_{-0.23}(\omega_{B_s}) \pm 0.03(V_{cb}) \pm 0.02(m_c), & \text{PQCD}, \\ 0.63^{+0.17}_{-0.13}(\omega_{B_s}) \pm 0.03(V_{cb}) \pm 0.02(m_c), & \text{PQCD+Lattice}, \end{cases} \quad (61)$$

$$\mathcal{B}(B_s^0 \to D_s^- l^+ \nu_l) = \begin{cases} 1.97^{+0.88}_{-0.65}(\omega_{B_s}) \pm 0.08(V_{cb}) \pm 0.03(m_c), & \text{PQCD}, \\ 1.84^{+0.76}_{-0.50}(\omega_{B_s}) \pm 0.08(V_{cb}) \pm 0.03(m_c), & \text{PQCD+Lattice}, \end{cases} \quad (62)$$

$$\mathcal{B}(B_s^0 \to D_s^{*-}\tau^+\nu_\tau) = \begin{cases} 1.45^{+0.45}_{-0.39}(\omega_{B_s}) \pm 0.06(V_{cb}) \pm 0.06(m_c), & \text{PQCD}, \\ 1.20^{+0.25}_{-0.22}(\omega_{B_s}) \pm 0.05(V_{cb}) \pm 0.02(m_c), & \text{PQCD+Lattice}, \end{cases} \tag{63}$$

$$\mathcal{B}(B_s^0 \to D_s^{*-}l^+\nu_l) = \begin{cases} 5.04^{+1.60}_{-1.41}(\omega_{B_s}) \pm 0.20(V_{cb}) \pm 0.16(m_c), & \text{PQCD}, \\ 4.42^{+1.26}_{-0.98}(\omega_{B_s}) \pm 0.17(V_{cb}) \pm 0.06(m_c), & \text{PQCD+Lattice}, \end{cases} \tag{64}$$

where the theoretical errors come mainly from the uncertainties of the input parameters $\omega_{B_s} = 0.50 \pm 0.05$ GeV, $|V_{cb}| = (42.2 \pm 0.8) \times 10^{-3}$ and $m_c = 1.275^{+0.025}_{-0.035}$ GeV. Errors from the uncertainties of the decay constants of the initial B_s and the final $D_s^{(*)}$ mesons are small and have been neglected. In Table 2, we list our PQCD and "PQCD+

Lattice" predictions of the branching ratios of the semileptonic decays of B_s^0, where the total errors are obtained by adding the individual errors in quadrature. As a comparison, we also show predictions of some other theoretical approaches in the SM framework. Unfortunately, there are no experimental results available at present. In Table 3, we show the theoretical predictions of the ratios
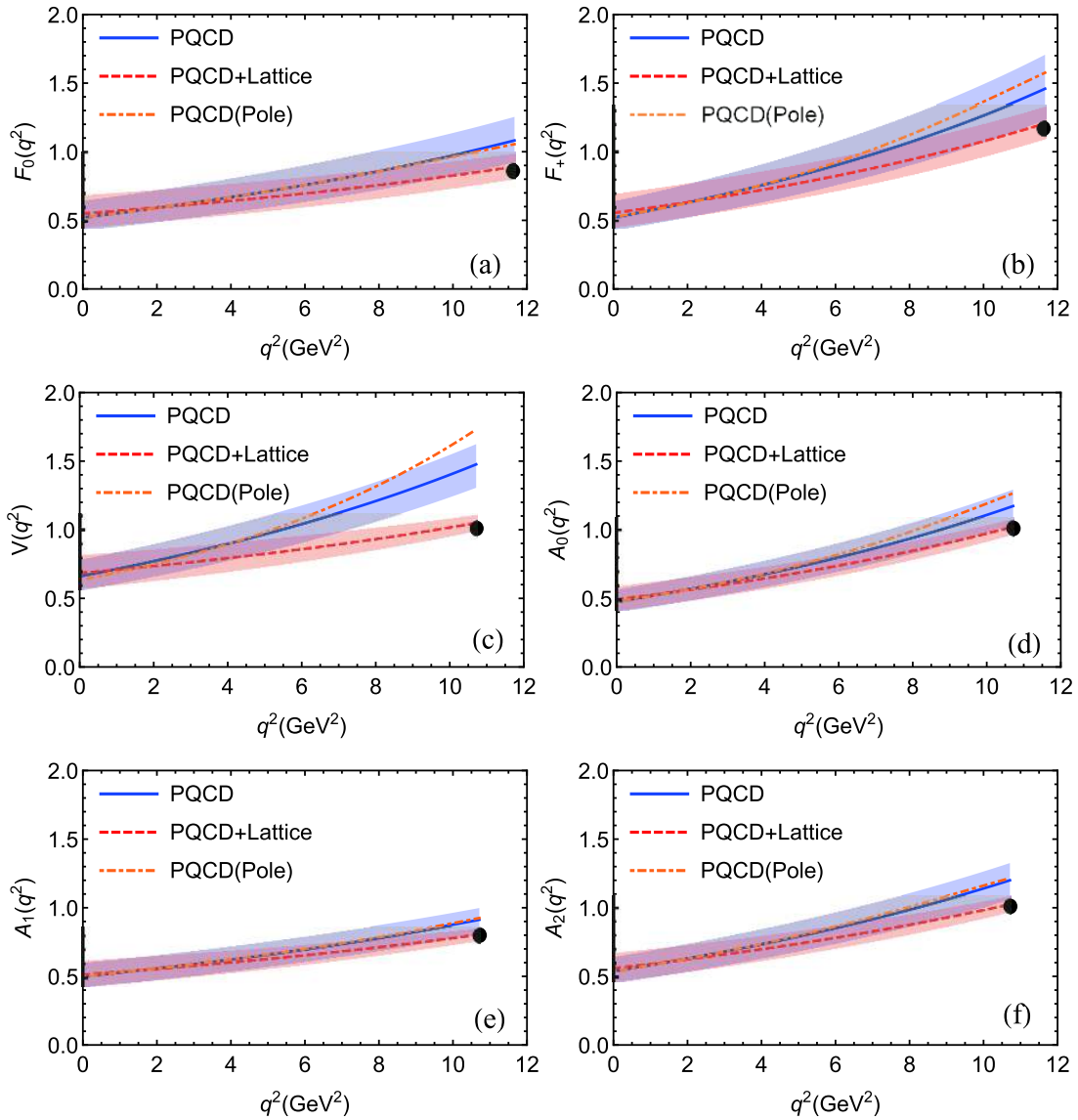

Fig. 2.   (color online) Theoretical predictions of the q^2 dependence of the six form factors for $B \to (D, D^*)$ transitions in the PQCD approach (blue solid curves) and the "PQCD+Lattice" method (red dashed curves) using the BCL parametrization [49, 50]. The orange dashed curves denote the PQCD predictions using the traditional pole model [9, 42, 58].

Fig. 3.   (color online) Theoretical predictions of the q^2 dependence of the six form factors for $B_s^0 \to (D_s^-, D_s^{*-})$ transitions in the PQCD approach (blue solid curves) and the "PQCD+Lattice" method (red dashed curves) using the BCL parametrization [49, 50]. The orange dashed curves denote the PQCD predictions using the traditional pole model [9, 42, 58].
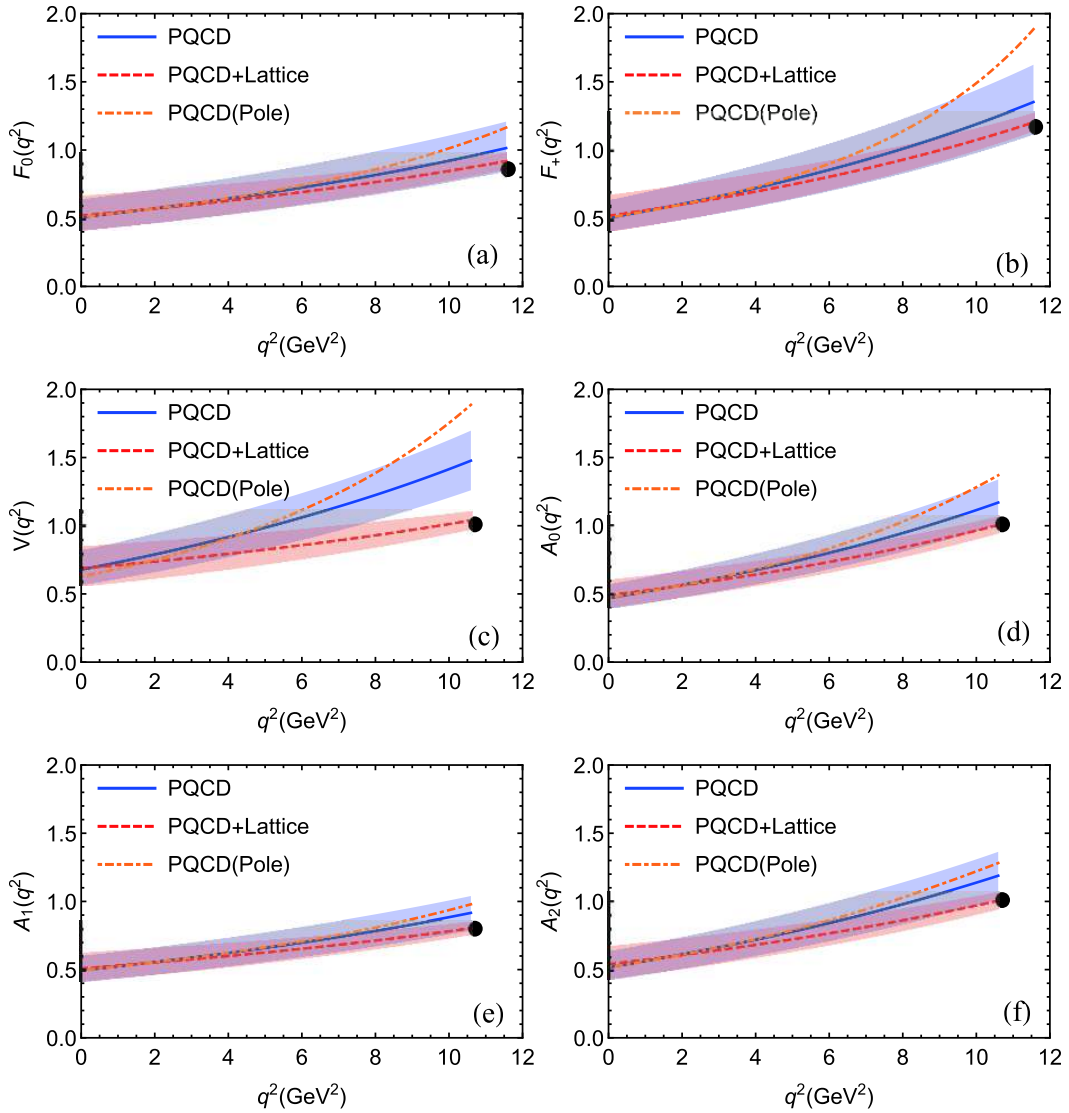
of the branching fractions $R(D_s)$ and $R(D_s^*)$ defined in the same way as $R(D^{(*)})$:

$$R(D_s) = \frac{\mathcal{B}(B_s^0 \to D_s^- \tau^+ \nu_\tau)}{\mathcal{B}(B_s^0 \to D_s^- l^+ \nu_l)}$$
$$= \begin{cases} 0.365^{+0.009}_{-0.012}, & \text{PQCD,} \\ 0.341^{+0.024}_{-0.025}, & \text{PQCD + Lattice,} \end{cases} \quad (65)$$

$$R(D_s^*) = \frac{\mathcal{B}(B_s^0 \to D_s^{*-} \tau^+ \nu_\tau)}{\mathcal{B}(B_s^0 \to D_s^{*-} l^+ \nu_l)}$$
$$= \begin{cases} 0.287^{+0.008}_{-0.011}, & \text{PQCD,} \\ 0.271^{+0.015}_{-0.016}, & \text{PQCD + Lattice,} \end{cases} \quad (66)$$

where l denotes an electron or a muon.

Following the same procedure as for B_s decays, we

calculate the branching ratios and the ratios $R(D^{(*)})$ for $B \to (D, D^*)(l^+ \nu_l, \tau^+ \nu_\tau)$ decays. The numerical results are listed in Table 4 for the branching ratios and in Table 5 for the ratios $R(D)$ and $R(D^*)$. In the estimate of the errors, $\omega_B = 0.40 \pm 0.04$ GeV was used.

From Tables 2 – 5, the following points can be noted:

(1) For the semileptonic decays $B \to D^{(*)} l^+ \nu_l$ with $l = (e, \mu, \tau)$, the "PQCD+Lattice" predictions of the branching ratios and the ratios $R(D^{(*)})$ agree with the available experimental data within errors. This can be viewed as evidence of the reliability of the "PQCD+Lattice" method for calculating semileptonic decays of B meson.

(2) For the four B_s decay modes and the eight B decay modes, the "PQCD+Lattice" predictions of the

Table 2.   Theoretical predictions (in units of 10^{-2}) of the branching ratios of the semileptonic decays of B_s^0, with $l = (e, \mu)$, obtained using various theoretical approaches [42, 67–73].

Approach	$\mathcal{B}(B_s^0 \to D_s^- l^+ \nu_l)$	$\mathcal{B}(B_s^0 \to D_s^- \tau^+ \nu_\tau)$	$\mathcal{B}(B_s^0 \to D_s^{*-} l^+ \nu_l)$	$\mathcal{B}(B_s^0 \to D_s^{*-} \tau^+ \nu_\tau)$
PQCD	$1.97^{+0.89}_{-0.66}$	$0.72^{+0.32}_{-0.23}$	$5.04^{+1.62}_{-1.43}$	$1.45^{+0.46}_{-0.40}$
PQCD+Lattice	$1.84^{+0.77}_{-0.51}$	$0.63^{+0.17}_{-0.13}$	$4.42^{+1.27}_{-1.00}$	$1.20^{+0.26}_{-0.23}$
PQCD[42]	$2.13^{+1.12}_{-0.77}$	$0.84^{+0.38}_{-0.28}$	$4.76^{+1.87}_{-1.49}$	$1.44^{+0.51}_{-0.42}$
IAMF[67]	$1.4 - 1.7$	$0.47 - 0.55$	$5.1 - 5.8$	$1.2 - 1.3$
RQM[68]	2.1 ± 0.2	0.62 ± 0.05	5.3 ± 0.5	1.3 ± 0.1
LCSR[69]	$1.0^{+0.4}_{-0.3}$	$0.33^{+0.14}_{-0.11}$	–	–
LFQM[70]	–	–	5.2 ± 0.6	$1.3^{+0.2}_{-0.1}$
CQM[71]	$2.73 - 3.00$	–	$7.49 - 7.66$	–
QCDSR[72]	$2.8 - 3.8$	–	$1.89 - 6.61$	–
Lattice[73]	$2.013 - 2.469$	$0.619 - 0.724$	–	–

Table 3.   Theoretical predictions of the ratios $R(D_s)$ and $R(D_s^*)$ obtained using various theoretical approaches [42, 68–70, 73].

Ratios	PQCD	PQCD+Lattice	PQCD[42]	RQM[68]	LCSR[69]	LFQM[70]	Lattice[73]
$R(D_s)$	$0.365^{+0.009}_{-0.012}$	$0.341^{+0.024}_{-0.025}$	$0.392(22)$	0.295	0.33	–	$0.299^{+0.027}_{-0.022}$
$R(D_s^*)$	$0.287^{+0.008}_{-0.011}$	$0.271^{+0.015}_{-0.016}$	$0.302(11)$	0.245	–	0.25	–

Table 4.   PQCD and "PQCD+Lattice" predictions of the branching ratios (in units of 10^{-2}) of the eight semileptonic decays $B \to D^{(*)} \tau^+ \nu_\tau$ and $B \to D^{(*)} l^+ \nu_l$ with $l = (e, \mu)$. As a comparison, the previous "PQCD+Lattice" predictions [10], the SM predictions based on HQET [11], and the world average of the measured values given in PDG 2018 [65] are also shown.

Channels	PQCD	PQCD+Lattice	PQCD[10]	HQET[11]	PDG[65]
$B^+ \to D^0 \tau^+ \nu_\tau$	$0.86^{+0.34}_{-0.25}$	$0.69^{+0.21}_{-0.17}$	$0.95^{+0.37}_{-0.31}$	0.66 ± 0.05	0.77 ± 0.25
$B^+ \to D^0 l^+ \nu_l$	$2.29^{+0.91}_{-0.72}$	$2.10^{+0.85}_{-0.62}$	$2.19^{+0.99}_{-0.76}$	–	2.20 ± 0.10
$B^+ \to D^{*0} \tau^+ \nu_\tau$	$1.60^{+0.39}_{-0.37}$	$1.34^{+0.26}_{-0.23}$	$1.47^{+0.43}_{-0.40}$	1.43 ± 0.05	1.88 ± 0.20
$B^+ \to D^{*0} l^+ \nu_l$	$5.53^{+1.45}_{-1.25}$	$4.89^{+1.21}_{-1.00}$	$4.87^{+1.60}_{-1.41}$	–	4.88 ± 0.10
$B^0 \to D^- \tau^+ \nu_\tau$	$0.82^{+0.33}_{-0.24}$	$0.62^{+0.19}_{-0.14}$	$0.87^{+0.34}_{-0.28}$	0.64 ± 0.05	1.03 ± 0.22
$B^0 \to D^- l^+ \nu_l$	$2.19^{+0.91}_{-0.68}$	$1.95^{+0.77}_{-0.56}$	$2.03^{+0.92}_{-0.70}$	–	2.20 ± 0.10
$B^0 \to D^{*-} \tau^+ \nu_\tau$	$1.53^{+0.37}_{-0.35}$	$1.25^{+0.25}_{-0.21}$	$1.36^{+0.38}_{-0.37}$	1.29 ± 0.06	1.67 ± 0.13
$B^0 \to D^{*-} l^+ \nu_l$	$5.32^{+1.37}_{-1.20}$	$4.63^{+1.15}_{-0.95}$	$4.52^{+1.44}_{-1.31}$	–	4.88 ± 0.10

branching ratios are generally smaller than the conventional PQCD predictions, but the differences are relatively small, less than 20%. The predictions also agree with the previous PQCD predictions given in Refs. [9, 10, 42] within the still large theoretical uncertainties.

(3) For the ratios $R(D_s)$ and $R(D_s^*)$, the theoretical errors largely cancel, and the PQCD and "PQCD+Lattice" predictions have a very small error, only about 5%. These predictions could be tested in the near future by the LHCb and Belle-II experiments.

(4) For the branching ratios, the predictions of the different theoretical approaches can be somewhat different for the same decay mode, but they still agree within errors, since the theoretical uncertainties are large. For the ratios $R(D)$ and $R(D^*)$, our "PQCD+Lattice" predictions agree with the average of the SM predictions obtained by HQET and the lattice QCD input for the form factors [3–6, 29].

(5) Comparing the two sets of ratios $(R(D), R(D_s))$ and $(R(D^*), R(D_s^*))$, listed in Tables 3 and 5, one can see that the $SU(3)$ flavor symmetry is well preserved in the PQCD and the "PQCD+Lattaice" approaches. This point could also be tested by experiments.

3.3 $P_\tau(D_{(s)}^{(*)})$, $F_L(D_{(s)}^{(*)})$ and $A_{FB}(\tau)$

Besides the branching ratios and the ratios $R(X)$, we consider three additional physical observables: the longitudinal polarization of the tau lepton $P_\tau(D_{(s)}^{(*)})$, the fraction of $D_{(s)}^*$ longitudinal polarization $F_L(D_{(s)}^*)$ and the forward-backward asymmetry of the tau lepton $A_{FB}(\tau)$. These quantities could be measured by the LHCb and Belle experiments, and may be sensitive to new physics [2, 31,

Table 5.   PQCD and "PQCD+Lattice" predictions of the ratios $R(D)$ and $R(D^*)$. As a comparison, the previous "PQCD+Lattice" predictions given in Ref. [10], the average of the SM predictions given in Ref. [29], measured values reported by the BaBar, Belle and LHCb collaborations [1, 24, 25], and the world averaged results from HFLAV group [29] are also shown.

Ratios	PQCD	PQCD+Lattice	PQCD[10]	SM[29]	BaBar[1]	Belle[24]	LHCb[25]	HFLAV[29]
$R(D)$	$0.376^{+0.011}_{-0.012}$	$0.324^{+0.020}_{-0.022}$	0.337(38)	0.299(3)	0.440(72)	0.307(40)	–	0.340(30)
$R(D^*)$	$0.288^{+0.008}_{-0.010}$	$0.272^{+0.013}_{-0.014}$	0.269(21)	0.258(5)	0.332(30)	0.283(23)	0.291(35)	0.295(14)

Table 6.   PQCD and "PQCD+Lattice" predictions of $P_\tau(D^{(*)}_{(s)})$, $F_L(D^*_{(s)})$ and $A_{FB}(\tau)$. The SM predictions and the measured values are also listed.

Observable	Approach	$B^0 \to D^- \tau^+ \nu_\tau$	$B^0_s \to D^-_s \tau^+ \nu_\tau$	$B^0 \to D^{*-} \tau^+ \nu_\tau$	$B^0_s \to D^{*-}_s \tau^+ \nu_l$
$P_\tau(D^{(*)}_{(s)})$	PQCD	0.32(1)	0.31(1)	−0.54(1)	−0.54(1)
	PQCD+Lat.	0.30(1)	0.30(1)	−0.53(1)	−0.53(1)
	SM[31]	–	–	−0.497(13)	–
	SM[32]	0.325(3)	–	−0.508(4)	–
	Belle[20]	–	–	$-0.38 \pm 0.51^{+0.21}_{-0.16}$	–
$F_L(D^*_{(s)})$	PQCD	–	–	0.42(1)	0.42(1)
	PQCD+Lat.	–	–	0.43(1)	0.43(1)
	SM[33]	–	–	0.457(10)	–
	SM[32]	–	–	0.441(6)	–
	Belle[30]	–	–	$0.60 \pm 0.08 \pm 0.04$	–
$A_{FB}(\tau)$	PQCD	0.35(1)	0.36(1)	−0.085(2)	−0.083(2)
	PQCD+Lat.	0.36(1)	0.36(1)	−0.054(2)	−0.050(2)
	SM[32]	0.361(1)	–	−0.084(13)	–

61–63]. Investigation of these physical observables may provide new clues for understanding the $R(D^{(*)})$ puzzle, and it is therefore necessary and interesting to calculate them.

In Refs. [31–33], these three physical observables were calculated in the SM framework, and possible new physics effects were studied. We calculate these observables in the PQCD and "PQCD+Lattice" approaches using Eqs. (44)-(59), and show the numerical predictions of $P_\tau(D^{(*)}_{(s)})$, $F_L(D^*_{(s)})$ and $A_{FB}(\tau)$ in Table 6. The measured values of $P_\tau(D^*)$ and $F_L(D^*)$ [20, 21, 30] given in Eqs. (4), (5) are also listed in Table 6. As a comparison, we also show the SM predictions of these physical observables given in Refs. [31, 32] .

From the results listed in Eqs. (4), (5) and in Table 6, the following points can be noted:

(1) The uncertainties of the theoretical predictions of the physical observables $P_\tau(D^{(*)}_{(s)})$, $F_L(D^*_{(s)})$ and $A_{FB}(\tau)$ are very small compared to the branching ratios, since the theoretical uncertainties largely cancel in the ratios.

(2) The PQCD and "PQCD+Lattice" predictions of the physical observables $P_\tau(D^{(*)}_{(s)})$, $F_L(D^*_{(s)})$ and $A_{FB}(\tau)$ for $B_{(s)} \to D_{(s)} \tau^+ \nu_\tau$ decays are very similar: the difference for a fixed decay mode is less than 5%. For $A_{FB}(\tau)$ of the $B_{(s)} \to D^*_{(s)} \tau^+ \nu_\tau$ decays, however, the difference is about 40%. The reason is the definition of the angular coeffi-

cient function $b^{(D^*)}_\theta(q^2)$, where the term $(H^2_{V,+} - H^2_{V,-})$ in Eq. (59) can be moderately changed by the high q^2 behavior of the form factors in the PQCD and "PQCD+Lattice" approaches. Clearly, a precise experimental measurement of the forward-backward asymmetry $A_{FB}(\tau)$ in the $B_{(s)} \to D^*_{(s)} l^+ \nu_l$ decays could be of great help to test and improve the factorization models.

(3) For $P_\tau(D^*)$ and $F_L(D^*)$, our theoretical predictions agree with the measured data within errors, partially due to the still large experimental errors. For all decay modes considered, the PQCD and "PQCD+Lattice" predictions of the three physical observables are consistent with the other approaches in the SM framework. We expect that these physical observables could be measured with high precision in the future by the LHCb and Belle-II experiments, which could help to test the theoretical models or approaches.

4   Summary

In this paper, we studied the semileptonic decays $B_{(s)} \to D^{(*)}_{(s)} l^+ \nu_l$ in the SM framework by employing the conventional PQCD factorization approach and the "PQCD+Lattice" approach. In the second approach, we took into account the lattice QCD results of the relevant form factors as input for the extrapolation from the low q^2

to the endpoint $q^2_{\max}$. We calculated the form factors $F_{0,+}(q^2)$, $V(q^2)$ and $A_{0,1,2}(q^2)$ of the $B_{(s)} \to D^{(*)}_{(s)}$ transitions, provided the theoretical predictions of the branching ratios of the B/B_s semileptonic decays and of the ratios $R(D^{(*)})$ and $R(D^{(*)}_s)$. In addition, we also gave our theoretical predictions of the additional physical observables: the longitudinal polarization of the tau lepton $P_\tau(D^{(*)}_{(s)})$, the fraction of $D^*_{(s)}$ longitudinal polarization $F_L(D^*_{(s)})$ and the forward-backward asymmetry of the tau lepton $A_{FB}(\tau)$.

From the numerical calculations and phenomenological analysis we noted the following points:

(1) For the twelve B/B_s semileptonic decay modes considered, the "PQCD+Lattice" predictions of the branching ratios are generally smaller than the conventional PQCD predictions, but the differences are relatively small, less than 20%. The "PQCD+Lattice" predictions of the branching ratios and the ratios $R(D^{(*)})$ agree with the available experimental measurements within errors.

(2) For the ratios $R(D_s)$ and $R(D^*_s)$, the PQCD and "PQCD+Lattice" predictions are the following:

$$R(D_s) = \begin{cases} 0.365^{+0.009}_{-0.012}, & \text{PQCD}, \\ 0.341^{+0.024}_{-0.025}, & \text{PQCD} + \text{Lattice}, \end{cases} \tag{67}$$

$$R(D^*_s) = \begin{cases} 0.287^{+0.008}_{-0.011}, & \text{PQCD}, \\ 0.271^{+0.015}_{-0.016}, & \text{PQCD} + \text{Lattice}. \end{cases} \tag{68}$$

They agree with the other SM predictions based on different approaches. These predictions could be tested by the LHCb and Belle-II experiments.

(3) For most of the observables $P_\tau(D^{(*)}_{(s)})$, $F_L(D^*_{(s)})$ and $A_{FB}(\tau)$, the PQCD and "PQCD+Lattice" predictions agree, and the difference is less than 5%. The relatively large difference of $A_{FB}(\tau)$ in the $B_{(s)} \to D^*_{(s)}\tau^+\nu_\tau$ decays can be reasonably explained.

(4) For $P_\tau(D^*)$ and $F_L(D^*)$, our theoretical predictions agree with the measurements within errors. For all decay modes considered, the PQCD and "PQCD+Lattice" predictions of these physical observables are consistent with the results of the other approaches in the SM framework. The LHCb and Belle-II experiments could help to test the above theoretical predictions.

Appendix: Relevant functions

In this appendix, we present the explicit expressions for some functions which have already appeared in the previous sections. The hard functions h_1 and h_2 come form the Fourier transform and can be written as:

$$\begin{aligned} h_1(x_1,x_2,b_1,b_2) =&K_0(\beta_1 b_1)[\theta(b_1-b_2)I_0(\alpha_1 b_2)K_0(\alpha_1 b_1) \\ &+\theta(b_2-b_1)I_0(\alpha_1 b_1)K_0(\alpha_1 b_2)]S_t(x_2), \end{aligned} \tag{A1}$$

$$\begin{aligned} h_2(x_1,x_2,b_1,b_2) =&K_0(\beta_2 b_1)[\theta(b_1-b_2)I_0(\alpha_2 b_2)K_0(\alpha_2 b_1) \\ &+\theta(b_2-b_1)I_0(\alpha_2 b_1)K_0(\alpha_2 b_2)]S_t(x_2), \end{aligned} \tag{A2}$$

where K_0 and I_0 are the modified Bessel functions, and

$$\alpha_1 = m_{B_{(s)}}\sqrt{x_2 r\eta^+}, \quad \alpha_2 = m_{B_{(s)}}\sqrt{x_1 r\eta^+ - r^2 + r^2_c}, \quad \beta_1 = \beta_2 = m_{B_{(s)}}\sqrt{x_1 x_2 r\eta^+}. \tag{A3}$$

The threshold resummation factor $S_t(x)$ is adopted from Ref. [74]:

$$S_t = \frac{2^{1+2c}\Gamma(3/2+c)}{\sqrt{\pi}\Gamma(1+c)}[x(1-x)]^c, \tag{A4}$$

and here we use $c = 0.3$.

The factor $\exp[-S_{ab}(t)]$ contains the Sudakov logarithmic corrections and the renormalization group evolution effects of the wave functions and the hard scattering amplitude with $S_{ab}(t) = S_B(t) + S_M(t)$ [74, 75],

$$S_B(t) = s\left(x_1\frac{m_{B_{(s)}}}{\sqrt{2}}, b_1\right) + \frac{5}{3}\int_{1/b_1}^{t}\frac{\mathrm{d}\bar{\mu}}{\bar{\mu}}\gamma_q(\alpha_s(\bar{\mu})), \tag{A5}$$

$$\begin{aligned} S_M(t) =&s\left(x_2\frac{m_{B_{(s)}}}{\sqrt{2}}r\eta^+, b_2\right) + s\left((1-x_2)\frac{m_{B_{(s)}}}{\sqrt{2}}r\eta^+, b_2\right) \\ &+ 2\int_{1/b_2}^{t}\frac{\mathrm{d}\bar{\mu}}{\bar{\mu}}\gamma_q(\alpha_s(\bar{\mu})), \end{aligned} \tag{A6}$$

where η^+ is defined in Eq. (7). The hard scale t and the quark anomalous dimension $\gamma_q = -\alpha_s/\pi$ govern the aforementioned renormalization group evolution. The explicit expressions for the functions $s(Q,b)$ can be found in Appendix A of Ref. [75]. The hard scales t_i in Eqs. (22)-(27) are chosen as the largest scales of virtuality of internal particles in the hard b quark decay diagram,

$$\begin{aligned} t_1 &= \max\{m_{B_{(s)}}\sqrt{x_2 r\eta^+}, 1/b_1, 1/b_2\}, \\ t_2 &= \max\{m_{B_{(s)}}\sqrt{x_1 r\eta^+ - r^2 + r^2_c}, 1/b_1, 1/b_2\}. \end{aligned} \tag{69}$$

References

1 J. P. Lees *et al.* (BABAR Collaboration), Phys. Rev. Lett., **109**: 101802 (2012)

2 J. P. Lees *et al.* (BABAR Collaboration), Phys. Rev. D, **88**: 072012 (2013)

3 D. Bigi and P. Gambino, Phys. Rev. D, **94**: 094008 (2016)

4 F. U. Bernlochner, Z. Ligeti, M. Papucci *et al.*, Phys. Rev. D, **95**: 115008 (2017)

5 S. Jaiswal, S. Nandi, and S.K. Patra, JHEP, **1712**: 060 (2017)

6 D. Bigi, P. Gambino, and S. Schacht, JHEP, **1711**: 061 (2017)

7 J. A. Bailey *et al.* (Fermilab Lattice and MILC Collaborations),

Phys. Rev. D, **92**: 034506 (2015)

8   H. Na *et al*. (HPQCD Collaboration), Phys. Rev. D, **92**: 054510 (2015)
9   Y. Y. Fan, W. F. Wang, S. Cheng *et al*., Chin. Sci. Bull., **59**: 125 (2014)
10   Y. Y. Fan, Z. J. Xiao, R. M. Wang *et al*., Sci. Bull., **60**: 2009 (2015)
11   S. Fajfer, J. F. Kamenik, and I. Nisandzic, Phys. Rev. D, **85**: 094025 (2012)
12   A. Datta, M. Duraisamy, and D. Ghosh, Phys. Rev. D, **86**: 034027 (2012)
13   Y. Sakaki, M. Tanaka, A. Tayduganov *et al*., Phys. Rev. D, **91**: 114028 (2015)
14   M. Freytsis, Z. Ligeti, and J. T. Ruderman, Phys. Rev. D, **92**: 054018 (2015)
15   S. Bhattacharya, S. Nandi, and S. K. Patra, Phys. Rev. D, **93**: 034011 (2016)
16   X.-Q. Li, Y.-D. Jang, and X. Zhang, JHEP, **1608**: 054 (2016)
17   D. Bardhan, P. Byakti, and D. Ghosh, JHEP, **1701**: 125 (2017)
18   A. Celis, M. Jung, X.-Q. Li *et al*., Phys. Lett. B, **771**: 168 (2017)
19   M. Huschle *et al*. (Belle Collaboration), Phys. Rev. D, **92**: 072014 (2015)
20   S. Hirose *et al*. (Belle Collaboration), Phys. Rev. Lett., **118**: 211801 (2017)
21   S. Hirose *et al*. (Belle Collaboration), Phys. Rev. D, **97**: 012004 (2018)
22   R. Aaij *et al*. (LHCb Collaboration), Phys. Rev. Lett., **120**: 171802 (2018)
23   A. Abdesselam *et al.* (Belle Collaboration), arxiv: 1904.08794[hep-ex]
24   G. Caria *et al.* (Belle Collaboration), arxiv: 1910.05864[hep-ex]
25   R. Aaij *et al*. (LHCb Collaboration), Phys. Rev. D, **97**: 072013 (2018)
26   G. Caria *et al.* (Belle Collaboration), talk given at 54th Rencontres de Moriond, EW, Mar. 22, 2019
27   A. Hicheur (LHCb Collaboration), arXiv: 1910.13121[hep-ex]
28   Y. Amhis *et al*. (HFLAV Collaboration), Eur. Phys. J. C, **77**: 895 (2017)
29   Y. Amhis *et al.* (HFLAV Collaboration), arXiv: 1909.12524[hep-ex]; and references therein
30   A. Abdesselam *et al.* (Belle Collaboration), arXiv: 1903.03102[hep-ex]
31   M. Tanaka and R. Watanabe, Phys. Rev. D, **87**: 034028 (2013)
32   Z. R. Huang, Y. Li, C. D. Lü *et al*., Phys. Rev. D, **98**: 095018 (2018)
33   S. Bhattacharya, S. Nandi, and S. K. Patra, Eur. Phys. J. C, **79**: 268 (2019)
34   S. Faller, A. Khodjamirian, Ch. Klein *et al*., Eur. Phys. J. C, **60**: 603 (2009)
35   Y. M. Wang, Y. B. Wei, Y. L. Shen *et al*., JHEP, **1706**: 062 (2017)
36   Y. Zhang, T. Zhong, X. G. Wu *et al*., Eur. Phys. J. C, **78**: 76 (2018)
37   T. Bhattacharya *et al*. (LANL/SWME Collaboration), arXiv: 1812.07675
38   Jon A. Bailey *et al*. (LANL-SWME Collaboration), EPJ Web Conf., **175**: 13012 (2018)
39   T. Kaneko *et al.* (JLQCD Collaboration), arXiv: 1811.00794
40   C. J. Monahan, C. M. Bouchard, G. P. Lepage *et al*. (HPQCD Collaboration), Phys. Rev. D, **98**: 114509 (2018)
41   Judd Harrison *et al*. (HPQCD Collaboration), Phys. Rev. D, **97**: 054502 (2018)
42   Y. Y. Fan, W. F. Wang ,and Z. J. Xiao, Phys. Rev. D, **89**: 014030 (2014)
43   W. F. Wang and Z. J. Xiao, Phys. Rev. D, **86**: 114025 (2012)
44   W. M. Wang, M. Liu, and Z. J. Xiao, Phys. Rev. D, **87**: 097501 (2013)
45   Z. J. Xiao, Y. Y. Fan, W. F. Wang *et al*., Chin. Sci. Bull., **59**: 3787 (2014)
46   W .F. Wang, Y. Y. Fan, and Z. J. Xiao, Chin. Phys. C, **37**: 093102 (2013)
47   W. F. Wang, X. Yu, C. D. Lü *et al*., Phys. Rev. D, **90**: 094018 (2014)
48   X. Q. Hu, S. P. Jin, and Z. J. Xiao, Chin. Phys. C, **44**: 023104 (2020)
49   C. Bourrely, I. Caprini, and L. Lellouch, Phys. Rev. D, **79**: 013008 (2009)
50   D. Leljak, B. Melic, and M. Patra, JHEP, **05**: 094 (2019)
51   T. Kurimoto, H. N. Li, and A. I. Sanda, Phys. Rev. D, **67**: 054028 (2003)
52   Z. J. Xiao, W. F. Wang, and Y. Y. Fan, Phys. Rev. D, **85**: 094003 (2012)
53   R. H. Li, C. D. Lü, and H. Zou, Phys. Rev. D, **78**: 014018 (2008)
54   M. Beneke and Th. Feldmann, Nucl. Phys. B, **592**: 3 (2001)
55   Jon A. Bailey *et al*. (Fermilab Lattice and MILC Collaborations), Phys. Rev. D, **89**: 114504 (2014)
56   Jon A. Bailey *et al*. (Fermilab Lattice and MILC Collaborations), Phys. Rev. D, **85**: 114502 (2012)
57   M. Atoui, V. Morenas, D. Becirevic *et al*., Eur. Phys. J. C, **74**: 2861 (2014)
58   W. Wang, Y. L. Shen, and C. D. Lü, Phys. Rev. D, **79**: 054012 (2009)
59   G. Buchalla, A. J. Buras, and M. E. Lautenbacher, Rev. Mod. Phys., **68**: 1125 (1996)
60   R. H. Li, C. D. Lü, W. Wang *et al*., Phys. Rev. D, **79**: 014013 (2009)
61   M. A. Ivanov, Jurgen G. Korner, and C. T. Tran, Phys. Rev. D, **92**: 114022 (2015)
62   M. A. Ivanov, Jurgen G. Korner *et al*., Phys. Rev. D, **95**: 036021 (2017)
63   M. Tanaka and R. Watanabe, Phys. Rev. D, **82**: 034027 (2010)
64   Y. Sakaki, R. Watanabe, M. Tanaka, A. Tayduganov, Phys. Rev. D, **88**: 094012 (2013)
65   M. Tanabashi *et al*. (Particle Data Group), Phys. Rev. D, **98**: 030001 (2018)
66   V. Lubicz *et al*. (ETM Collaboration), Phys. Rev. D, **96**: 034524 (2017)
67   X. J. Chen, H. F. Fu, C. S. Kim *et al*., J. Phys. G, **39**: 045002 (2012)
68   R.N. Faustov and V.O. Galkin, Phys. Rev. D, **87**: 034033 (2013)
69   R. H. Li, C. D. Lu, and Y. M. Wang, Phys. Rev. D, **80**: 014005 (2009)
70   G. Li, F. L. Shao, and W. Wang, Phys. Rev. D, **82**: 094031 (2010)
71   S. M. Zhao, X. Liu, and S. J. Li, Eur. Phys. J. C, **51**: 601 (2007)
72   K. Azizi and M. Bayar, Phys. Rev. D, **78**: 054011 (2008); K. Azizi, Nucl. Phys. B, **801**: 70 (2008)
73   R. Dutta and N. Rajeev, Phys. Rev. D, **97**: 095045 (2018)
74   T. Kurimoto, H. N. Li, and A. I. Sanda, Phys. Rev. D, **65**: 014007 (2001)
75   C. D. Lü, K. Ukai, and M. Z. Yang, Phys. Rev. D, **63**: 074009 (2001)